Journal of Zhejiang University-SCIENCE A (Applied Physics & Engineering)
ISSN 1673-565X (Print); ISSN 1862-1775 (Online)
www.zju.edu.cn/jzus; www.springerlink.com
E-mail: jzus@zju.edu.cn

Experimental study of lightweight aggregate concrete under multiaxial stresses*

Han-yong LIU, Yu-pu SONG

(*Structural Engineering Institute, School of Civil Engineering, Faculty of Infrastructure Engineering, Dalian University of Technology, Dalian 116024, China*)

†E-mail: structliu@yahoo.com.cn; syupu@dlut.edu.cn

Received Oct. 15, 2009; Revision accepted Jan. 14, 2010; Crosschecked July 19, 2010

Abstract: Lightweight aggregate concrete cube specimens (100 mm×100 mm×100 mm) and plate specimens (100 mm×100 mm×50 mm) were tested under biaxial compression-compression (CC) and compression-tension (CT) load combinations. For comparison, normal concrete plate specimens (100 mm×100 mm×50 mm) were tested under the same load combinations. Based on the test results, a two-level strength criterion of lightweight aggregate concrete in both octahedral stress coordinate and principal stress coordinate was suggested. The lightweight aggregate concrete cube specimens (100 mm×100 mm×100 mm) were then tested under triaxial compression-compression-compression (CCC) load combination with corresponding tests on normal concrete cube specimens (100 mm×100 mm×100 mm). The effect of intermediate principal stress on triaxial compressive strength is further examined. A "plastic flow plateau" area was apparent in principal compressive stress-strain relationships of lightweight aggregate concrete but not in normal concrete. A quadratic formula was suggested for the expression of strength criterion under triaxial compression.

Key words: Lightweight aggregate concrete, Normal concrete, Biaxial loads, Triaxial loads, Compressive strength, Tensile strength, Stress-strain relationships, Plastic flow plateau, Lode angle

doi:10.1631/jzus.A0900619 **Document code:** A **CLC number:** TU5

1 Introduction

Lightweight aggregate concrete has obvious advantages of a higher strength/weight ratio, better tensile strain capacity, without alkali-aggregate reaction, lower coefficient of thermal expansion, and superior heat and sound insulation characteristics due to air voids in the lightweight aggregate (Jo *et al*., 2007; Mouli and Khelafi, 2007). By virtue of these advantages, lightweight aggregate concrete has been used for tall buildings, long-span bridges, offshore platforms, and marine structures (Haug and Fjeld, 1996; Melby *et al*., 1996; Liu *et al*., 2007). Many of the structural elements of the structures are essentially in a multiaxial state of stress.

The finite element method has been used for the analysis and design of complex structures, such as offshore oil platforms and nuclear containment structures. These types of structures cannot be treated properly by more approximate methods. The finite element method, however, requires a good understanding of the actual material behavior under different load combinations to yield accurate and realistic results. Therefore, a whole analytical idealization of lightweight aggregate concrete is desirable, and to achieve this understanding, the behavior of lightweight aggregate concrete under multiaxial stress must be examined.

For normal concrete, reasonable amounts of data are available (Wang *et al*., 1987; Imran and Pantazopoulou, 1996; Nielsen, 1998; Li and Ansari, 2000; Li *et al*., 2002; Lim and Nawy, 2005; He and Song,

* Project (No. 50679007) supported by the National Natural Science Foundation of China

2008). This is not the case for lightweight aggregate concrete. In fact, several researchers (Taylor *et al*., 1972; Atan and Slate, 1973; Hussein and Marzouk, 2000) have studied the behavior of lightweight aggregate concrete subjected to biaxial stresses. The experimental programs covered the whole range of biaxial loading (compression-compression (CC), compression-tension (CT), and tension-tension (TT)). On the other hand, to the best of our knowledge, there is no published data concerning the behavior of lightweight aggregate concrete under triaxial states of stress.

The objectives of the current experiments include testing both lightweight aggregate concrete and normal concrete cube and plate specimens under biaxial CC and CT load combinations. With this data, a two-level strength criterion of lightweight aggregate concrete in octahedral stress coordinate and principal stress coordinate is suggested. A further objective is to test these materials under triaxial compression-compression-compression (CCC) load combinations.

2 Experimental

2.1 Triaxial test apparatus

The specimens were tested in a specially designed triaxial test apparatus (Fig. 1). The triaxial test apparatus consisted of three identical loading frames. The three loading axes were not connected to each other, and could act completely independent. Each loading axis consisted of four steel screw rods, fixed in a rectangular configuration between two rigid steel end platens. To eliminate the friction between the specimen and the loading platen, brush-type loading platens can be used. For the same purpose, other methods, such as normal loading platens with three 2-mm resin sheets with grease, can also be used. The triaxial loading on the specimens was provided by means of three servo-controlled CT actuators with a maximum compression capacity of 2500 kN and a maximum tension capacity of 500 kN. A close-loop system in displacement control was utilized. The displacement control was provided by means of an external ultra-precision alternating current (AC) linear variable displacement transducer (LVDT). The experimental data were acquired and processed by computer. Fig. 2 shows the test setup under loading conditions.

Fig. 1 Dynamic-static triaxial electronic hydraulic servo test system

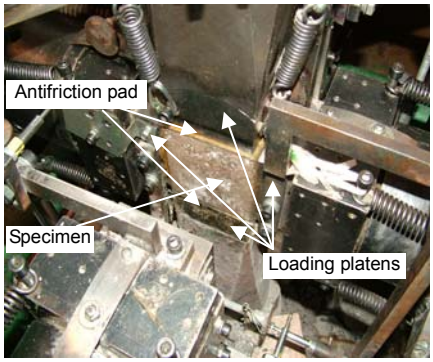

Fig. 2 Test setup under loading conditions

2.2 Test specimens

The lightweight aggregate concrete cube and plate specimens were 100 mm×100 mm×100 mm and 100 mm×100 mm×50 mm in dimension, respectively. The lightweight aggregate concrete cube specimens were subjected to all three stress combinations including CC, CT and CCC. The lightweight aggregate concrete plate specimens were subjected to CC and CT stress combinations only. The normal concrete cube and plate specimens were tested as comparison. The normal concrete cube specimens were subjected to CCC stress combination and the normal concrete plate specimens were subjected to CC and CT stress combinations.

For the lightweight aggregate concrete mixture, a gangue-based lightweight aggregate was used as coarse aggregate. The physical and mechanical properties of the coarse aggregate are shown in Table 1. The lightweight aggregates were pre-soaked with water for 1 h before mixing. The mixture proportion of lightweight aggregate concrete was 1:0.42:1.22: 0.98 (Portland cement:water:fluvial sand:coarse aggregate).

Table 1 Physical and mechanical properties of lightweight aggregate

Grain size (mm)	Bulk density (kg/m^3)	Water-absorption capacity in 1 h (%)	Crushing strength (MPa)	Apparent density (kg/m^3)	Porosity (%)
5–15	693	18.7	4.2	1227	43.5

The lightweight aggregate concrete cube strength at testing was 23.83 MPa without reducing friction and the uniaxial compressive strength was 16.68 MPa. The uniaxial tensile strength of lightweight aggregate concrete was 1.75 MPa. The dry apparent density and Young's modulus of lightweight aggregate concrete were 1531 kg/m^3 and 1.41×10^4 MPa, respectively.

Crushed limestone was used as coarse aggregate for the normal concrete. The mixture proportion of normal concrete was 1:0.52:1.59:3.56 (Portland cement:water:fluvial sand:crushed limestone). The normal concrete cube strength at testing was 25 MPa without reducing friction and the uniaxial compressive strength was 20 MPa. The dry apparent density and Young's modulus of normal concrete were 2215 kg/m^3 and 2.53×10^4 MPa, respectively. All the specimens were tested after 28 d.

All the specimens were cast in steel molds. During casting, the normal concrete specimens were compacted by a vibrating table. The lightweight aggregate concrete specimens were compacted artificially after a short time on a vibrating table to prevent the lightweight aggregates from floating on the surface of the specimens. The casting surfaces were finished and the specimens were placed under a plastic cover to avoid drying out. Twenty-four hours after casting, the specimens were demolded and placed in a humidity room with 99% relative humidity and a constant temperature of (20±2) °C. The specimens were taken out of the humidity room 2 d before testing, and then ground and prepared for testing. The six sides of the specimens were ground to ensure that the specimen had flat edges and right-angle corners. The grinder employed a wet-type grinding method using a diamond grinding wheel. The final ground surface finish was within ±0.1 mm.

2.3 Reducing friction

Previous testing results for friction reduction by Wang *et al*. (1987) showed that a fluorine-based resin (Teflon) was a comparatively suitable material. Three 2-mm resin sheets with grease of MoS_2 were used as a friction-reducing pad in this study.

2.4 Loading method for tensile test

For the tensile test, the tensile side of the specimen and the loading were platen bonded together at the joints with building structural adhesive (Fig. 3). The tensile strength and the shear strength of the building structural adhesive were 30 and 17.5 MPa, respectively. For a firm connection, the unsubstantial layer of the tensile sides must be worn off and the tensile sides must have flat edges and right-angle corners.

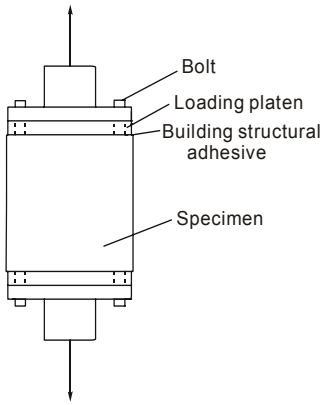

Fig. 3 Loading method for tensile test

2.5 Loading rate

A displacement control method was used in this test. The displacement control was provided by means of an external ultra-precision AC LVDT. The loading rate was 0.002 mm/s in the direction of σ_1 for the tests which had tensile loading. It was 0.01 mm/s in the direction of σ_3 for the multiaxial compression tests. The loads of another two directions were applied according to the stress ratio which was preset. The loading rate was controlled by a computer.

3 Test results and analysis of biaxial concrete strength

3.1 Test results

The test results of lightweight aggregate concrete and normal concrete under biaxial CC and CT load combinations are shown in Tables 2 and 3,

respectively. Note that notations for the principal stresses and strains are $\sigma_1 \geq \sigma_2 \geq \sigma_3$, $\varepsilon_1 \geq \varepsilon_2 \geq \varepsilon_3$, σ_i and ε_i are negative in compression and positive in tension. The stress ratio α is σ_2/σ_3 ($\alpha>0$, $\sigma_1=0$) in the biaxial compression region, and the stress ratio α is σ_1/σ_3 ($\alpha<0$, $\sigma_2=0$) in the combined compression and tension region. In Tables 2 and 3, the uniaxial compressive strengths of lightweight aggregate concrete and normal concrete are f_{lc} (=−16.68 MPa) and f_{nc} (=−20 MPa), respectively. The relative ratios of biaxial strength to uniaxial strength are σ_3/f_{lc} for lightweight aggregate concrete and σ_3/f_{nc} for normal concrete, respectively.

Table 2 Biaxial testing of lightweight aggregate concrete

Specimen dimension (mm)	Stress ratio	Specimen quantity	σ_3 (MPa)	σ_3/f_{lc}
100×100×100	0.25	3	−20.98	1.26
100×100×50	0.25	4	−20.68	1.24
100×100×100	0.50	3	−21.30	1.28
100×100×50	0.50	3	−21.35	1.28
100×100×100	0.75	3	−20.08	1.20
100×100×50	0.75	3	−20.72	1.24
100×100×100	1.00	4	−21.22	1.27
100×100×50	1.00	3	−21.20	1.27
100×100×100	−0.05	4	−9.69	0.58
100×100×50	−0.05	3	−9.80	0.59
100×100×100	−0.10	3	−6.33	0.38
100×100×50	−0.10	3	−7.00	0.42
100×100×100	−0.25	3	−4.99	0.30
100×100×50	−0.25	3	−4.79	0.29
100×100×100	−0.50	3	−3.60	0.22
100×100×50	−0.50	3	−3.26	0.20
100×100×100	−0.75	3	−2.64	0.16
100×100×50	−0.75	4	−1.97	0.12
100×100×100	−1.00	4	−1.72	0.10
100×100×50	−1.00	3	−1.70	0.10

Table 3 Biaxial testing of normal concrete

Specimen dimension (mm)	Stress ratio	Specimen quantity	σ_3 (MPa)	σ_3/f_{nc}
100×100×50	0.25	4	−25.2	1.26
100×100×50	0.50	4	−28.0	1.40
100×100×50	0.75	3	−26.4	1.32
100×100×50	1.00	5	−26.9	1.35
100×100×50	−0.05	3	−15.6	0.78
100×100×50	−0.25	3	−5.2	0.26
100×100×50	−0.50	3	−2.8	0.14
100×100×50	−0.75	3	−2.0	0.10
100×100×50	−1.00	4	−1.6	0.08

In general, the ultimate strength of concrete under biaxial compression is higher than that under uniaxial compression due to the increased confinement from biaxial compression. The strength increase under biaxial compression is dependent on the biaxial stress ratio. The maximum biaxial strength occurs at a biaxial stress ratio of 0.5 for all specimens tested. At this stress ratio, the strength increases about 28% for lightweight aggregate concrete and 40% for normal concrete, respectively.

The effect of aggregate type on the biaxial behavior of concrete can be demonstrated by comparing the lightweight aggregate concrete mixture with the normal concrete mixture. The lightweight aggregate concrete indicated a lower strength gain than for the normal concrete at all stress ratios except 0.25. At the stress ratio of 0.25, the lightweight aggregate concrete indicated the same strength increase as normal concrete of about 26%. This contradicts the findings by Hussein and Marzouk (2000) that the high-strength lightweight aggregate concrete with a cylindrical compressive strength of 61.8 MPa indicated a higher strength gain than the high-strength normal concrete with a cylindrical compressive strength of 71.1 MPa.

In the biaxial CT region, introducing an absolute value of stress ratios increases the compressive strength decreases, and the tensile strength increases. The compressive strength and tensile strength under biaxial CT load combination, however, are lower than that under uniaxial loading. There is a significant difference in the behavior between lightweight aggregate concrete and normal concrete. At the absolute value of stress ratio of 0.05, the value of σ_3/f_{lc} is less than that of σ_3/f_{nc}. When the absolute value of stress ratio is higher than 0.05, however, the value of σ_3/f_{lc} is larger than that of σ_3/f_{nc} (Tables 2 and 3).

3.2 Failure modes

The crack patterns and failure modes were observed for all the test specimens. In general, there was no fundamental difference in the crack patterns and failure modes owing to the use of lightweight aggregates under different biaxial loading combinations.

Under biaxial compression, and at the low stress ratio of 0.25, the specimen showed formation of microcracks parallel to both the free surface and the direction of σ_3. Failure occurred, however, by the formation of a major crack that had an angle of 20° to

30° to the free surface of the specimen (Fig. 4a). For specimens subjected to biaxial compression ratios of 0.5, 0.75, and 1, failure occurred by the formation of a splitting crack that was inclined at an angle of 10° to 20° to the direction of the applied load (Fig. 4b). These failure modes were observed for both the lightweight aggregate concrete and the normal concrete.

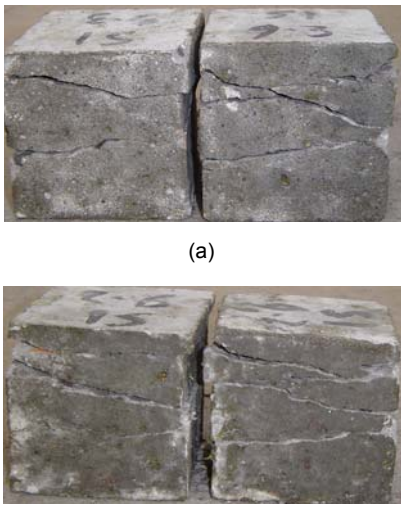

(a)

(b)

Fig. 4 Failure modes of lightweight aggregate concrete under biaxial compression

(a) α=0.25 (surface under the action of σ_3); (b) α=0.5 (surface under the action of σ_3)

The tests under combined compression and tension revealed that only one continuous crack perpendicular to the principal tensile stress was formed. The failure surfaces of lightweight aggregate concrete specimens revealed that the cracks passed through the coarse aggregate and the mortar (Fig. 5a). Examination of the failure surfaces of normal concrete specimens, however, showed that there were few cracks passed directly through the coarse aggregate, instead almost all the cracks passed mainly through the mortar (Fig. 5b).

3.3 Strength criterion

The tests results under different biaxial loading combinations in $\sigma_{oct}/|f_{lc}|$ and $\tau_{oct}/|f_{lc}|$ coordinate are shown in Fig. 6, where σ_{oct} and τ_{oct} are the octahedral normal stress and octahedral shear stress, respectively. The results of the relations between $\sigma_{oct}/|f_{lc}|$ and $\tau_{oct}/|f_{lc}|$ can regress in a two-level line. The first level is from the uniaxial compression state of stress ($\sigma_{oct}/|f_{lc}|$=−0.33, $\tau_{oct}/|f_{lc}|$=0.47) to the biaxial compression state of stress. The second level is from the uniaxial compression state of stress to the combined compression and tension state of stress and the uniaxial tension stress state ($\sigma_{oct}/|f_{lc}|$=0.035, $\tau_{oct}/|f_{lc}|$=0.046). A two-level strength criterion is suggested.

CC state of stress:

$$\begin{aligned}&\tau_{oct}/|f_{lc}|=0.397-0.218\sigma_{oct}/|f_{lc}|,\\&\sigma_{oct}/|f_{lc}|\le -0.33.\end{aligned}\tag{1}$$

CT state of stress:

$$\begin{aligned}&\tau_{oct}/|f_{lc}|=0.086-1.153\sigma_{oct}/|f_{lc}|,\\&-0.33\le\sigma_{oct}/|f_{lc}|\le 0.035.\end{aligned}\tag{2}$$

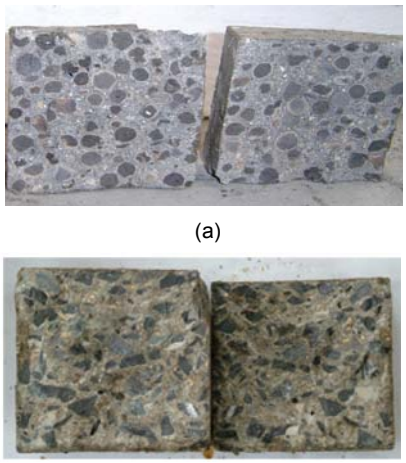

(a)

(b)

Fig. 5 Failure modes of lightweight aggregate concrete (a) and normal concrete (b) under CT loading combinations

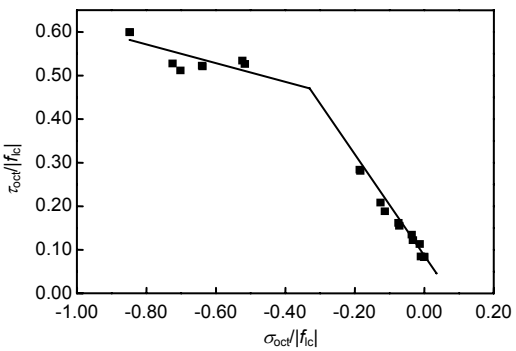

Fig. 6 Test results under CC and CT loading combinations of lightweight concrete with octahedral coordinate

A strength criterion in principal stress coordinate can be deduced from the above strength criterion.

CC state of stress:

$$\sigma_3/|f_{lc}|=1.191/[0.218(1+\alpha)-\sqrt{2}(1-\alpha+\alpha^2)^{1/2}],$$
$$\sigma_2/|f_{lc}|=\alpha\sigma_3/|f_{lc}|,\quad \alpha\geq 0. \tag{3}$$

CT state of stress:

$$\sigma_3/|f_{lc}|=0.258/[1.153(1+\alpha)-\sqrt{2}(1-\alpha+\alpha^2)^{1/2}],$$
$$\sigma_1/|f_{lc}|=\alpha\sigma_3/|f_{lc}|,\quad -\infty\leq\alpha\leq 0.$$
$$\text{or } \sigma_1/|f_{lc}|=0.258/[1.153(1+1/\alpha)+\sqrt{2}(1-1/\alpha+1/\alpha^2)^{1/2}]. \tag{4}$$

4 Test results and analysis of triaxial concrete strength

4.1 Test results

The test results of triaxial compressive strength of lightweight aggregate concrete and normal concrete are shown in Tables 4 and 5, respectively. Note that notations for the principal stresses and strains are $\sigma_1\geq\sigma_2\geq\sigma_3$, $\varepsilon_1\geq\varepsilon_2\geq\varepsilon_3$, σ_i and ε_i are negative in compression and positive in tension. In Tables 4 and 5, the uniaxial compressive strength of lightweight aggregate concrete and normal concrete is f_{lc} (=−16.68 MPa) and f_{nc} (=−20 MPa), respectively. The relative ratios of triaxial strength to uniaxial strength are σ_3/f_{lc} for lightweight aggregate concrete and σ_3/f_{nc} for normal concrete, respectively.

When $\sigma_1/\sigma_3\geq 0.30$, $\sigma_2/\sigma_3\geq 0.50$, a "plastic flow plateau" area (stress is a constant or has a very small increase, but strain has a sudden increase) is presented in the principal compressive stress-strain relationships of lightweight aggregate concrete (Fig. 7). After the "plastic flow plateau" area, the stress continued to increase with the increase of the strain, like a "stress-intensity". When the specimen was at failure, there was a large value of peak strain. For example, at the stress ratios σ_1/σ_3=0.30, σ_2/σ_3=0.50, the principal compressive strain was 0.16.

In fact, in the "plastic flow plateau" area, the inner structures of the lightweight aggregate concrete are already destroyed. Under the action of the high-compressive stress, the mortar frames are

Table 4 Triaxial compression test of lightweight aggregate concrete

Stress ratio σ_3:σ_2:σ_1	Specimen quantity	σ_3 (MPa)	σ_3/f_{lc}	Peak strength (MPa)
1:0.10:0.10	3	−28.17	1.69	−28.17
1:0.25:0.10	5	−31.49	1.89	−31.49
1:0.30:0.10	8	−31.00	1.86	−31.00
1:0.50:0.10	3	−34.75	2.08	−34.75
1:0.75:0.10	3	−31.80	1.91	−31.80
1:1.00:0.10	3	−30.32	1.82	−30.32
1:0.25:0.25	4	−42.34	2.54	−42.34
1:0.30:0.25	3	−45.19	2.71	−45.19
1:0.50:0.25	5	−48.31	2.90	−48.31
1:0.75:0.25	4	−43.90	2.63	−43.90
1:1.00:0.25	3	−39.09	2.34	−39.09
1:0.30:0.30	3	−50.66	3.04	−50.66
1:0.50:0.30	3	−51.05	3.06	−111.24
1:1.00:0.30	3	−47.38	2.84	−96.55
1:0.50:0.50	5	−58.86	3.53	−118.03
1:0.75:0.50	4	−51.47	3.09	−129.30
1:1.00:0.50	3	−51.31	3.08	−123.30
1:0.75:0.75	3	−55.94	3.35	−180.59
1:1.00:0.75	4	−50.70	3.04	−156.76
1:1.00:1.00	3	−57.74	3.46	Non-failure

Table 5 Triaxial compression test of normal concrete

Stress ratio σ_3:σ_2:σ_1	Specimen quantity	σ_3 (MPa)	σ_3/f_{nc}
1:0.10:0.10	4	−52.43	2.62
1:0.25:0.10	4	−73.60	3.68
1:0.30:0.10	4	−71.77	3.59
1:0.50:0.10	6	−70.20	3.51
1:0.75:0.10	5	−62.13	3.11
1:1.00:0.10	4	−61.71	3.09
1:0.25:0.25	4	−149.35	7.47
1:0.30:0.25	3	−188.01	9.40
1:0.50:0.25	3	−187.28	9.36
1:0.75:0.25	3	Non-failure	Non-failure
1:1.00:0.25	3	−176.17	8.81
1:0.50:0.30	3	Non-failure	Non-failure
1:0.75:0.50	3	Non-failure	Non-failure

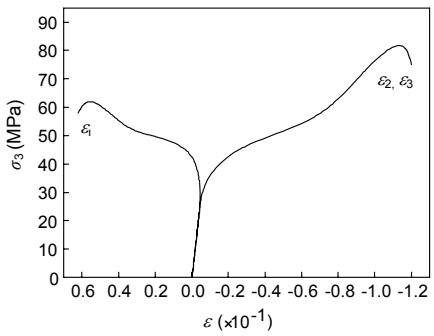

Fig. 7 Stress-strain relationships of lightweight concrete (σ_3:σ_2:σ_1=1:1:0.3)

destroyed first, and then the lightweight aggregates undergo pressure and become destroyed. The failures of mortar frames and lightweight aggregates lead to a large deformation, so that the stress-strain relationships of lightweight aggregate concrete presents a "plastic flow plateau" area. After the stress redistribution, the inner interspaces of lightweight aggregate concrete specimens are compacted, and then an additional load can be applied on the specimens, like a "stress-intensity" of metal. The "stress-intensity" of lightweight aggregate concrete, however, is different from the "stress-intensity" of metal. Under this condition, the lightweight aggregates and the mortar are already crushed, so that when $\sigma_1/\sigma_3 \geq 0.3$, $\sigma_2/\sigma_3 \geq 0.5$, the stress of the "plastic flow plateau" area ought to be the ultimate strength of lightweight aggregate concrete, but not the peak stress. The test results of the stress of "plastic flow plateau" area and the peak stress of lightweight aggregate concrete are shown in Table 4. The stresses of the "plastic flow plateau" area are not significantly dependent on the stress ratio as shown in Table 4. They are all in the range of 47.38–58.86 MPa.

In this study, there was no "plastic flow plateau" area in the principal compressive stress-strain relationships of normal concrete, even under high stress ratios, owing to the low power of the test apparatus. It can be predicted that a "plastic flow plateau" area will be present in the principal compressive stress-strain relationships of normal concrete under high stress ratios when the test apparatus can provide enough power.

4.2 Strength criterion at equal lateral stresses

As shown in Table 4, it is found that at the equal lateral stresses $\sigma_1=\sigma_2=0.10\sigma_3$, $0.25\sigma_3$, and $0.3\sigma_3$, the values of σ_3 are $1.69f_{lc}$, $2.54f_{lc}$, and $3.04f_{lc}$, respectively; at the equal lateral stresses $\sigma_1=\sigma_2=0.50\sigma_3$, $0.75\sigma_3$, and σ_3, the values of σ_3 are $3.53f_{lc}$, $3.35f_{lc}$, and $3.46f_{lc}$, respectively. The relation between σ_3 and $\sigma_1=\sigma_2$ is nearly bilinear (Fig. 8). A bilinear strength criterion of triaxial compressive strength at the equal lateral stress ratios is suggested:

$$\sigma_3 / f_{lc} = 1.38 + 1.83\sigma_2 / f_{lc},$$
$$0 \leq \sigma_2 / \sigma_3 = \sigma_1 / \sigma_3 \leq 0.33,$$
$$\sigma_3 / f_{lc} = 3.44,$$
$$0.33 \leq \sigma_2 / \sigma_3 = \sigma_1 / \sigma_3 \leq 1.00. \quad (5)$$

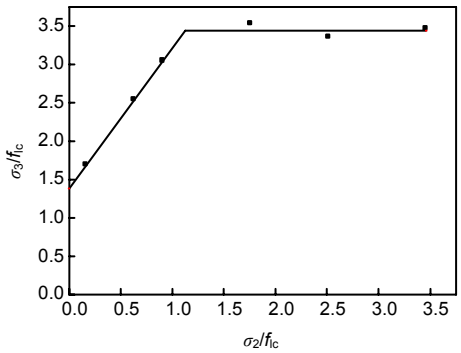

Fig. 8 Relationships between the ratios of σ_3/f_{lc} and σ_2/f_{lc} for lightweight aggregate concrete under equal lateral stresses ($\sigma_1=\sigma_2$)

As shown in Fig. 9, at the same stress ratios of σ_1/σ_3, the introduction of stress ratios σ_2/σ_3 significantly affects the values of σ_3/f_{lc}. For instance, when the stress ratio $\sigma_1/\sigma_3=0.30$ and σ_2/σ_3 is small, the values of σ_3/f_{lc} increase with the increase values of σ_2/σ_3. When the values of σ_2/σ_3 become larger, the increase in the value of σ_3/f_{lc} initially becomes less and when the values of σ_2/σ_3 are over 0.33, the values of σ_3/f_{lc} starts to decrease. Thus, for triaxial compression of $\sigma_1>\sigma_2>\sigma_3$ the intermediate stress σ_2 significantly affects the value of σ_3 under high ratios of σ_1/σ_3. When the value of σ_1/σ_3 is small, however, such as $\sigma_1/\sigma_3 \leq 0.10$, the effect is not very significant. There is a difference in the behavior between lightweight aggregate concrete and normal concrete. As shown in Fig. 10, at the stress ratio $\sigma_1/\sigma_3=0.10$, the intermediate stress σ_2 already significantly affects the value of σ_3 for normal concrete.

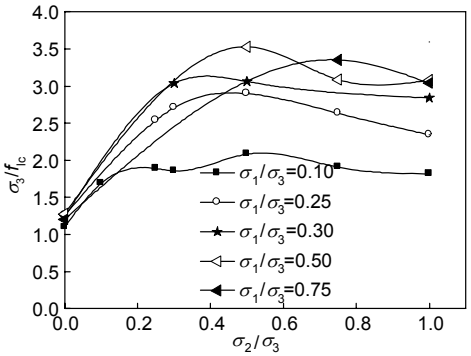

Fig. 9 Variations of the strength ratios of σ_3/f_{lc} under different ratios of σ_2/σ_3 for lightweight aggregate concrete

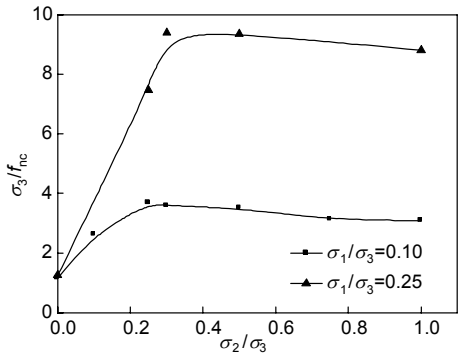

Fig. 10 Variations of the strength ratios of σ_3/f_{nc} under different ratios of σ_2/σ_3 for normal concrete

4.3 Strength characteristics on deviatoric plane

The octahedral normal stress σ_{oct}, octahedral shear stress τ_{oct} and lode angle θ can be calculated from the test results as shown in Table 4. The relationships between $\tau_{oct}/|f_{lc}|$ and θ are shown in Fig. 11. At the low and middle stress ratios ($0<\sigma_1/\sigma_3<0.30$, $0<\sigma_2/\sigma_3<0.50$), the minimum value of τ_{ot} (note that $\tau_{ot}=\tau_{oct}/|f_{lc}|$ is the relative ratio of octahedral shear stress τ_{oct} to uniaxial compressive strength on tensile meridian) is obtained on the tensile meridian. The values of τ_{oct} increase with the increase of the values of θ. The maximum value of τ_{oc} (note that $\tau_{oc}=\tau_{oct}/|f_{lc}|$ is the relative ratio of octahedral shear stress τ_{oct} to uniaxial compressive strength on compressive meridian) is obtained on the compressive meridian. The values of τ_{ot}/τ_{oc} increase with the increase absolute values of $\sigma_{oct}/|f_{lc}|$. They are in the range of 0.78–1.00.

At high stress ratios ($\sigma_1/\sigma_3\geq0.30$, $\sigma_2/\sigma_3\geq0.50$), the values of τ_{ot} are approximately equal to those of τ_{oc} because the stresses of the "plastic flow plateau" area are not significantly dependent on the stress ratios and they remain between 47.38–58.86 MPa. Then, at high stress ratios, $\tau_{oc}=\tau_{ot}$ is assumed in our experiments.

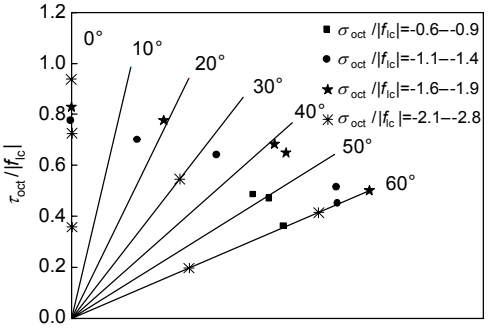

Fig. 11 Relationships between octahedral shear stress and lode angle

4.4 Strength characteristics on meridian

In a series of studies, experiments with lightweight aggregate concrete under triaxial CCT loading, triaxial compression-tension-tension (CTT) loading and triaxial tension-tension-tension (TTT) loading were also performed. The results are shown in Table 6. The values of $\sigma_{oct}/|f_{lc}|$ and $\tau_{oct}/|f_{lc}|$ can be calculated from the test results as shown in Tables 4 and 6. The relationships between $\sigma_{oct}/|f_{lc}|$ and $\tau_{oct}/|f_{lc}|$ are shown in Fig. 12. The values of $\tau_{oct}/|f_{lc}|$ increased with the increase of the absolute values of $\sigma_{oct}/|f_{lc}|$ at low and middle stress ratios, but the values of $\tau_{oct}/|f_{lc}|$ decreased with the increase of the absolute value of $\sigma_{oct}/|f_{lc}|$ at high stress ratios. Due to the existence of a "plastic flow plateau" area, the meridians have intersection points with the hydrostatics compressive axis. This is different from the opening failure surface of normal concrete. The shapes of meridians can be roughly simulated with a quadratic parabola.

Table 6 Triaxial testing of lightweight aggregate concrete

Stress state	Stress ratio σ_3:σ_2:σ_1	Specimen quantity	σ_3 (MPa)	σ_1 (MPa)
CCT	−1:−1.00:0.25	5	−2.84	0.71
	−1:−1.00:0.75	3	−2.62	1.97
	−1:−1.00:1.00	6	−1.72	1.72
CTT	−1:0.05:.0.10	3	−4.10	0.41
	−1:0.10:0.50	4	−1.30	0.65
	−1:0.10:0.75	4	−1.15	0.86
	−1:0.10:1.00	3	−0.90	0.90
	−1:0.25:0.25	4	−2.30	0.58
	−1:0.75:0.75	3	−0.80	0.60
TTT	1:4.00:4.00	3	0.46	1.84
	1:2.00:2.00	3	1.23	2.46
	1:1.00:1.00	5	1.75	1.75

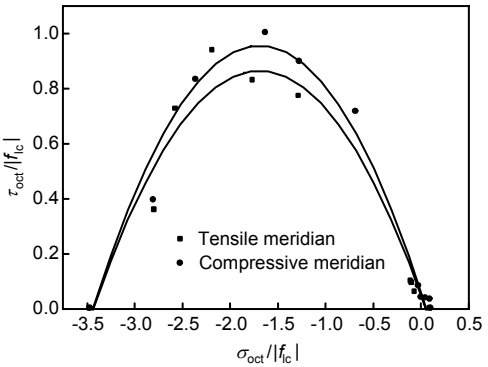

Fig. 12 Relationships between octahedral normal stress and octahedral shear stress on tensile meridian and compressive meridian

4.5 Strength criterion under triaxial stresses

According to the strength characteristics of lightweight aggregate concrete on deviatoric plane and meridian, the following formula can be used as the expression of strength criterion in the octahedral stress coordinate.

$$\tau_{\mathrm{oct}}(\theta)/|f_{\mathrm{lc}}| = \tau_{\mathrm{ot}}/|f_{\mathrm{lc}}| + (\tau_{\mathrm{oc}}/|f_{\mathrm{lc}}| - \tau_{\mathrm{ot}}/|f_{\mathrm{lc}}|)\sin^{\beta}(1.5\theta), \quad 0^\circ \le \theta \le 60^\circ, \tag{6}$$

where β is the influence coefficient of σ_{oct} and θ to $\tau_{\mathrm{oct}}(\theta)$.

$$\tau_{\mathrm{ot}}/|f_{\mathrm{lc}}| = a_{\mathrm{t}} + b_{\mathrm{t}}\sigma_{\mathrm{oct}}/|f_{\mathrm{lc}}| + c_{\mathrm{t}}(\sigma_{\mathrm{oct}}/|f_{\mathrm{lc}}|)^2, \tag{7}$$

$$\tau_{\mathrm{oc}}/|f_{\mathrm{lc}}| = a_{\mathrm{c}} + b_{\mathrm{c}}\sigma_{\mathrm{oct}}/|f_{\mathrm{lc}}| + c_{\mathrm{c}}(\sigma_{\mathrm{oct}}/|f_{\mathrm{lc}}|)^2, \tag{8}$$

where a_{t}, b_{t}, c_{t}, a_{c}, b_{c}, and c_{c} are parameters. According to the least square method, the test results in Fig. 12 can regress in Eqs. (7) and (8). Then the values of a_{t}, b_{t}, c_{t}, a_{c}, b_{c}, and c_{c} are obtained: $a_{\mathrm{t}}=5.755\times10^{-2}$, $b_{\mathrm{t}}=-9.8268\times10^{-1}$, $c_{\mathrm{t}}=-3.0878\times10^{-1}$, $a_{\mathrm{c}}=1.0922\times10^{-1}$, $b_{\mathrm{c}}=-1.08619$, and $c_{\mathrm{c}}=-3.4952\times10^{-1}$. Eqs. (7) and (8) are substituted into Eq. (6). Under triaxial compression, after adjustment, $\beta=3$ is determined. Then, the ultimate form of Eq. (6) is

$$\tau_{\mathrm{oct}}(\theta)/|f_{\mathrm{lc}}| = \tau_{\mathrm{ot}}/|f_{\mathrm{lc}}| + (\tau_{\mathrm{oc}}/|f_{\mathrm{lc}}| - \tau_{\mathrm{ot}}/|f_{\mathrm{lc}}|)\sin^{3}(1.5\theta), \quad 0^\circ \le \theta \le 60^\circ \tag{9}$$

where

$$\tau_{\mathrm{ot}}/|f_{\mathrm{lc}}| = 5.755\times10^{-2} - 9.8268\times10^{-1}\sigma_{\mathrm{oct}}/|f_{\mathrm{lc}}| - 3.0878\times10^{-1}(\sigma_{\mathrm{oct}}/|f_{\mathrm{lc}}|)^2, \tag{10}$$

$$\tau_{\mathrm{oc}}/|f_{\mathrm{lc}}| = 1.0922\times10^{-1} - 1.08619\sigma_{\mathrm{oct}}/|f_{\mathrm{lc}}| - 3.4952\times10^{-1}(\sigma_{\mathrm{oct}}/|f_{\mathrm{lc}}|)^2, \tag{11}$$

$$\theta = \arccos[(2\sigma_1 - \sigma_2 - \sigma_3)/(3\sqrt{2}\tau_{\mathrm{oct}})], \quad 0^\circ \le \theta \le 60^\circ. \tag{12}$$

The formula regressed by the test results considers both the influence of lode angle θ and the characteristics of "plastic flow plateau". As shown in Fig. 12, the regression is in good agreement with the test results.

5 Conclusions

The following conclusions can be obtained from the present investigation concerning the behavior of lightweight aggregate concrete under multiaxial stress:

1. The biaxial compressive strength of lightweight aggregate concrete is lower than that of normal concrete.

2. The lightweight aggregate concrete under biaxial compression loads indicates a strength increase of about 20%–28% greater than the uniaxial compressive strength. The tensile strength and compressive strength under combined biaxial compression and tension are lower than the uniaxial tensile and uniaxial compressive strength. Considering the scatter of the test results and the simplicity of use, a two-level strength criterion in octahedral stress coordinate and principal stress coordinate can be suggested.

3. Under triaxial compression, when $\sigma_1/\sigma_3\ge0.3$, $\sigma_2/\sigma_3\ge0.5$, a "plastic flow plateau" area present in the principal compressive stress-strain relationships of lightweight aggregate concrete. The stresses of the "plastic flow plateau" area are not significantly dependent on the stress ratio. They are in the range of 47.38–58.86 MPa.

4. For triaxial compression of $\sigma_1>\sigma_2>\sigma_3$, the intermediate stress σ_2 significantly affects the values of σ_3 under high ratios of σ_1/σ_3. Under low ratios of σ_1/σ_3, such as $\sigma_1/\sigma_3\le0.1$, however, the effect is not significant. There is a difference in the behavior between lightweight aggregate concrete and normal concrete. At the stress ratio of $\sigma_1/\sigma_3=0.1$, the intermediate stress σ_2 already significantly affects the values of σ_3.

5. A quadratic formula is suggested for the expression of strength criterion under triaxial compression. It considers both the influence of lode angle θ and the characteristics of "plastic flow plateau", and it is in good agreement with the test results.

References

Atan, Y., Slate, F.O., 1973. Structural lightweight concrete under biaxial compression. *ACI Journal, Proceedings*, **70**(3):182-186.

Haug, A.K., Fjeld, S., 1996. A floating concrete platform hull made of lightweight aggregate concrete. *Engineering Structures*, **18**(11):831-836. [doi:10.1016/0141-0296(95)00160-3]

He, Z.J., Song, Y.P., 2008. Failure mode and constitutive model of plain high-strength high-performance concrete under biaxial compression after exposure to high temperatures. *Acta Mechanica Solida Sinica*, **21**(2):149-159. [doi:10.1007/s10338-008-0818-1]

Hussein, A., Marzouk, H., 2000. Behavior of high-strength concrete under biaxial stresses. *ACI Materials Journal*, **97**(1):27-36.

Imran, I., Pantazopoulou, S.J., 1996. Experimental study of plain concrete under triaxial stress. *ACI Materials Journal*, **93**(6):589-601.

Jo, B.W., Park, S.K., Park, J.B., 2007. Properties of concrete made with alkali-activated fly ash lightweight aggregate (AFLA). *Cement & Concrete Composites*, **29**(2):128-135. [doi:10.1016/j.cemconcomp.2006.09.004]

Li, Q.B., Ansari, F., 2000. High-strength concrete in triaxial compression by different sizes of specimens. *ACI Materials Journal*, **97**(6):684-689.

Li, Q.B., Zhang, L.X., Ansari, F., 2002. Damage constitutive for high strength concrete in triaxial cyclic compression. *International Journal of Solids and Structures*, **39**(15): 4013-4025. [doi:10.1016/S0020-7683(02)00265-2]

Lim, D.H., Nawy, E.G., 2005. Behaviour of plain and steel-fibre-reinforced high-strength concrete under uniaxial and biaxial compression. *Magazine of Concrete Research*, **57**(10):603-610. [doi:10.1680/macr.2005.57.10.603]

Liu, H.Y., Wang, L.C., Song, Y.P., Wang, H.T., 2007. Experimental study on mechanical properties of steel fiber reinforced high-strength lightweight aggregate concrete. *Journal of Building Structures*, **28**(5):110-117 (in Chinese).

Melby, K., Jordet, E.A., Hansvold, C., 1996. Long-span bridges in Norway constructed in high-strength LWA concrete. *Engineering Structures*, **18**(11):845-849. [doi:10.1016/0141-0296(95)00158-1]

Mouli, M., Khelafi, H., 2007. Strength of short composite rectangular hollow section columns filled with lightweight aggregate concrete. *Engineering Structures*, **29**(8):1791-1797. [doi:10.1016/j.engstruct.2006.10.003]

Nielsen, C.V., 1998. Triaxial behavior of high-strength concrete and mortar. *ACI Materials Journal*, **95**(2):144-151.

Taylor, M.A., Jain, A.K., Ramey, M.R., 1972. Path dependent biaxial compressive testing of an all-lightweight aggregate concrete. *ACI Journal, Proceedings*, **69**(12): 758-764.

Wang, C.Z., Guo, Z.H., Zhang, X.Q., 1987. Experimental investigation of biaxial and triaxial compressive concrete strength. *ACI Materials Journal*, **84**(2):92-100.